The effect of stress ageing on deformation in thin films of polystyrene and poly(ether sulphone)

C. J. G. Plummer and A. M. Donald*
Cavendish Laboratory, Cambridge University, Department of Physics, Madingley Road, Cambridge CB3 0HE, UK
(Received 11 July 1990; revised 25 September 1990; accepted 5 October 1990)

Step-strain ridges are known to form when glassy polymers are subjected to a stepwise series of strain increments. For relatively short times between increments (ageing times) and at relatively low temperatures, these step-strain ridges (studied here in crazes in polystyrene and in deformation zones in poly(ether sulphone)) become more marked as the interval t_i between successive strain increments is increased. This is related to the phenomenon of stress ageing, as suggested by the approximate logarithmic dependence of the ridge height δ on t_i. However, at high temperatures, and or low molecular weight and relatively long t_i, δ may begin to *decrease* with t_i. This is argued to be a result of the onset of disentanglement in the aged material.

(Keywords: stress; deformation; crazing; ageing; film; polystyrene; poly(ether sulphone))

INTRODUCTION

During the early 1980s, the work of Donald and Kramer[1,2] demonstrated a link between the microstructure of deformation in a variety of glassy polymers and the entanglement network parameters. These latter could be deduced for each polymer from measurements of the shear modulus in the 'rubbery plateau' temperature regime above the glass transition temperature (T_g). In the entanglement network model, topological constraints on the relative motion of individual chains are treated analogously to chemical crosslinks. The polymer is idealized as a network of polymer strands of root-mean-square (r.m.s.) contour length l_e and molecular weight M_e, linked at so-called 'entanglement points', which have an r.m.s. spatial separation d_e. This suggests the existence of a 'natural draw ratio', $\lambda_{max} \sim l_e/d_e$, since, if the entanglement network remains immutable during deformation, strain hardening will set in as the strands between entanglement points become fully stretched[1,2].

In certain temperature regimes below T_g, regions of stable shear necking called deformation zones (DZs) form, with a uniform extension ratio λ_{DZ}, when thin films of the polymer are strained in tension[3,4]. In other temperature regimes, depending on the polymer in question, DZs are replaced by crazing as the characteristic mode of tensile deformation[1-7]. Crazes consist of a network of voids and highly drawn fibrils with an extension ratio λ_{craze}, whose value within the craze body is again uniform. Both λ_{DZ} and λ_{craze} are found to correlate well with λ_{max} for a wide variety of polymers (and consequently a large range of λ_{max}), with λ_{DZ} typically being approximately $0.6\lambda_{max}$ and λ_{craze} somewhat greater at $0.8\lambda_{max}$ (refs. 1, 2). This is strong evidence for the validity of the network model in the glassy state. Moreover, the difference between λ_{DZ} and λ_{craze} may be accounted for in terms of the network model, since the open voided structure of a craze requires that there be a certain degree of entanglement loss during craze formation[1,2]. The effect of this on the fibril extension ratio has been quantified for room-temperature (RT) polystyrene (PS) crazes using calculations based on the network model, and good agreement has been found between predicted and observed values of $\lambda_{craze}/\lambda_{DZ}$ (refs. 1, 8, 9).

Although the value of λ_{craze} in the craze body is essentially uniform, transmission electron microscopy (TEM) of crazes has revealed a region of higher λ, the 'midrib' at the centre of the craze[10]. The midrib is the remnant of the region of the craze that first forms at the craze tip as it advances, and it is believed that its higher extension ratio reflects the stress concentration known to exist at the craze tip[1,10,11]. This is argued to result in additional disruption to the entanglement network to that taking place in regions of the craze formed during subsequent widening, for which the drawing stress is lower.

Donald and Kramer investigated whether local increases in the extension ratio might also occur when a craze or a DZ is subjected to stepwise increments in strain[12]. They carried out a series of tests on thin films of PS and polycarbonate (PC) at RT, in which they applied successive 1% increments in strain to their samples at 1 min intervals. However, they found that, under these experimental conditions, both λ_{craze} and λ_{DZ} remained constant as a function of the number of strain increments, with the exception of a region of *lower* λ, corresponding to the position of the craze–bulk interface prior to each successive strain increment[12]. These ridges were identified with 'bulges' (i.e. regions which had thinned less) observed by Kramer previously in necks in nylon-6,10 that had been step-strained in a similar fashion[13].

In both cases, the phenomenon was attributed to stress ageing[13-17]. Kramer had previously showed that, at

* To whom correspondence should be addressed

0032-3861/91/183322-09

ageing stresses just below the 'propagation stress' for a neck at a given strain rate in nylon-6,10, the neck would continue to grow at a reduced rate, but that when the original propagation stress was reapplied, a delay time was observed between the application of the stress and the resumption of the original neck propagation rate[13]. The length of this delay time depended on the ageing stress. He was able to relate this behaviour to the appearance of a second yield point when the high stress was applied. This effect leads to relatively high stresses being required for further drawing in the neck compared with those in undeformed regions of the polymer, and thus after a certain ageing time one would expect it to be easier for fresh material away from the neck to draw in preference to material at the neck edge. This effect can account for the observed bulges[12].

More recent work has suggested that the phenomenon of stress ageing may be important for craze fibril stability[18]. It has been found that craze fibril breakdown in PS generally initiates in the so-called 'active zone' at the craze–bulk interface, where fresh polymer is drawn into the fibrils, and not in the more highly stretched midrib region. Chains in the newly formed regions of fibril are assumed to remain in the strain-softened state for some characteristic residence time t_r during which their mobility is sufficiently high for them to disentangle, that is, to escape their entanglement constraint by sliding past each other under the influence of the craze surface stress[6,7,18–22]. After a time τ_{dis}, called the disentanglement time[18,22], a given chain is eventually able to escape all the entanglements along its length and so is effectively no longer load-bearing, since loads can only be transferred via entanglement. Thus if $\tau_{dis} \leqslant t_r$ the fibril will fail.

Clearly t_r will be at least in part related to stress ageing, since it is the presence of the stress which confers mobility on the chains, but at the present time there is no *a priori* justification for any assumptions regarding its behaviour, particularly over wide ranges of temperature (T). (Stress ageing occurs when a sample that has been strained is maintained under finite stress when the strain rate is temporarily dropped to zero. It is found that a higher stress is then required to reinitiate deformation when the strain is increased again, and this phenomenon is known as stress ageing[13].) However Kramer's work[13], for example, suggests that t_r should be a strong function both of temperature and of the local stress conditions, and independent of molecular weight. The present study has been undertaken in order to gain some further insight into the stress ageing behaviour of craze fibrils, and thin films in general, by carrying out a systematic study of the effects of step-straining on the extension ratio of crazes in polystyrene (PS) and deformation zones (DZs) in poly(ether sulphone) (PES).

EXPERIMENTAL

We have examined the effect of step-straining in monodisperse PS (supplied by Polymer Laboratories and Alfa Products Ltd, with molecular weights M of 100 000, 300 000 and 1 150 000), polydisperse PS (supplied by BDH Chemicals Ltd, with a molecular weight average of 100 000 and a polydispersity of approximately 2) and polydisperse PES (Victrex, supplied by ICI plc, with molecular weight averages in the range 47 000 to 69 000 and a polydispersity of approximately 2).

Thin films, of the order of 0.6 μm in thickness, were made by letting a drop of a solution of the polymer in question fall from a syringe onto a rotating glass slide (the speed of rotation of the slide controlled the film thickness) and allowing the solvent to evaporate. When the solvent had evaporated the resulting film was floated off on a water bath and picked up on a copper grid that had been previously coated with the same polymer. After drying, the film was bonded to this grid by exposure to the appropriate solvent vapour[10]. The solvents were toluene for PS, and cyclohexanone at 40°C for PES. In order to ensure that the observed crazes or deformation zones had experienced the complete pattern of strain increments, it was necessary to introduce starter cracks into the samples. The presence of a starter crack ensured that successive strain increments were accommodated by the widening of pre-existing crazes or DZs rather than the nucleation of additional crazes or DZs (and if any subsequent nucleation did occur, these crazes/DZs could easily be identified and discounted). Such starter cracks were produced by indenting the film with a Vickers hardness indenter[23] prior to floating it off the glass slide. An array of diamond-shaped holes approximately 10 μm across, and with a period equal to the spacing of the copper grid, was thus introduced into each film and, with care, the films could then be picked up from the water bath so as to ensure that there was a crack at the centre of each grid square.

Once mounted on the copper grids the films were placed in a vacuum oven at 90°C and 190°C for PS and PES respectively, for a minimum of 1 h. This served both to dry the films and to ensure that subsequent shear deformation was localized in the PES films. Longer ageing treatments tended to promote crazing in PES at high temperature[7], which was unsuitable for systematic study since crazes in PES were found to be too brittle to accommodate large strains.

The films, bonded to their copper grids, were then strained at a constant strain rate in increments of approximately 2%, on a heating stage, while being observed using an optical microscope, which could be operated in both reflected and transmitted light. In order to investigate the effect of strain ageing, the time interval between each successive strain increment was varied over a range of different temperatures and at two different strain rates, 5×10^{-6} and $10^{-2}\ s^{-1}$. Subsequent to deformation and removal from the straining rig, the individual grid squares were examined using a JEOL 2000EX transmission electron microscope (TEM).

RESULTS

Figure 1 shows TEM micrographs of monodisperse PS $M = 300\,000$ crazes, which have been given successive strain increments of 2% at RT and at a strain rate of $10^{-2}\ s^{-1}$, with intervals t_i of 5 min, 1 min, 30 s and 20 s between each strain increment as indicated. For $t_i > 20$ s, dark lines may clearly be seen running approximately parallel to the craze–bulk interface, corresponding to the position of the craze–bulk interfaces after each strain increment. On the other hand, for $t_i = 20$ s no such lines can be seen and the craze microstructure is considerably coarser than for high t_i (*Figure 1d*) because the lack of time available for stress relaxation leads to widespread craze fibril breakdown. Evidence for this can be seen by

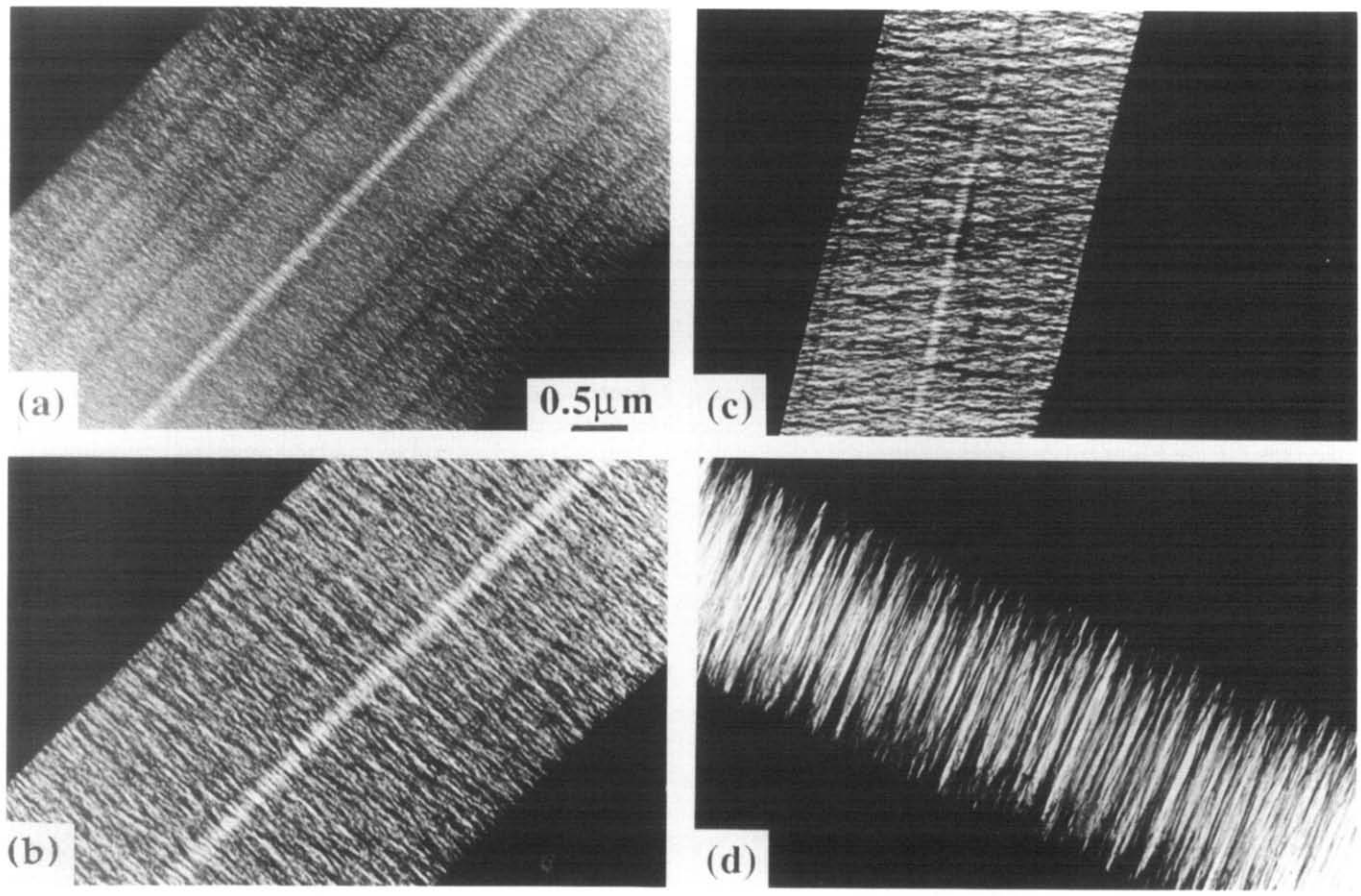

Figure 1 TEM micrographs of crazes in PS $M = 300\,000$ step-strained at room temperature and at a strain rate of $10^{-2}\,s^{-1}$ with various time intervals between strain increments: (a) $t_i = 5$ min; (b) $t_i = 1$ min; (c) $t_i = 30$ s; (d) $t_i = 20$ s

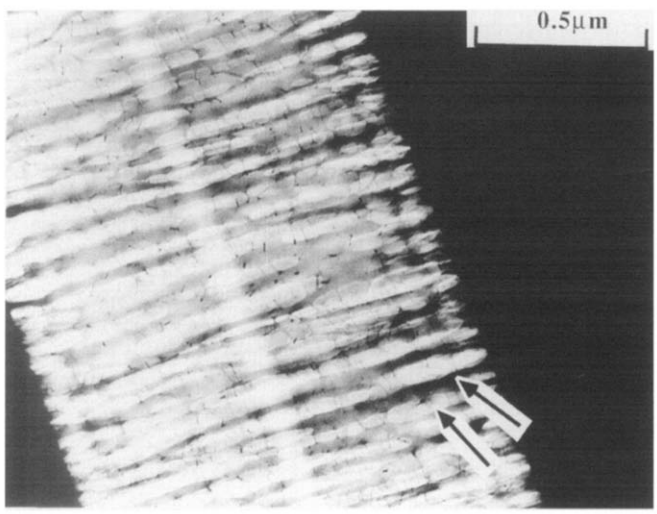

Figure 2 A craze in a 0.4 μm thick film of monodisperse PS $M = 1\,150\,000$, given five successive strain increments of 2% at RT and at a strain rate of $10^{-2}\,s^{-1}$ with $t_i = 5$ min. The positions of the two most prominent ridges are shown

close examination of *Figure 1d*, which reveals many misaligned damaged fibrils.

Figure 2 shows a craze in a 0.4 μm thick film of monodisperse PS $M = 1\,150\,000$, given successive strain increments of 2% at RT and at a strain rate of $10^{-2}\,s^{-1}$ with $t_i = 5$ min. In this film the craze microstructure is coarser than in the 0.6 μm films used in the systematic tests, owing to changes in the constraint on plastic deformation as the film thickness is decreased relative to the fibril separation[24]. Because of this it is possible to see individual fibrils rather clearly. It then becomes clear that the dark lines correspond to regions where the extension ratio of individual fibrils is relatively low; that is, on the scale of an individual fibril, these lines are exactly analogous to the bulges seen during the step-straining of macroscopic necks in nylon 6,10[13].

Since the optical density of the electron image plate is a decreasing function of the corresponding mass thickness of the sample, it is also possible to identify the dark lines with a decrease in the overall craze extension ratio λ_{craze}, as pointed out by Donald and Kramer[12]. The magnitude of these changes in λ_{craze} can be estimated using

$$\frac{1}{\lambda_{craze}} = 1 - \frac{\ln(\varphi_{craze}/\varphi_{film})}{\ln(\varphi_{hole}/\varphi_{film})} \qquad (1)$$

where φ_{craze}, φ_{film} and φ_{hole} are the optical densities of the craze, the film and a hole in the film as measured via microdensitometry of the electron image plate[10]. *Figure 3* shows the results obtained in this way for a RT craze in PS $M = 300\,000$ strained at a strain rate of $10^{-2}\,s^{-1}$ with $t_i = 5$ min (cf. *Figure 1a*), with the trace running from the craze–matrix interface ($x = 0$) to the midrib. Under these conditions, with the exception of the ridges, λ_{craze} is constant and approximately equal to 4 over the bulk of the craze, consistent with Donald and Kramer's earlier observations[12]. Measurement of the ratio $(\lambda_{craze} - \lambda_{ridge})/\lambda_{craze}$, hereafter termed δ, is approximately 0.05 ± 0.15. (It should be noted that, although a spread in λ values naturally occurs within any single

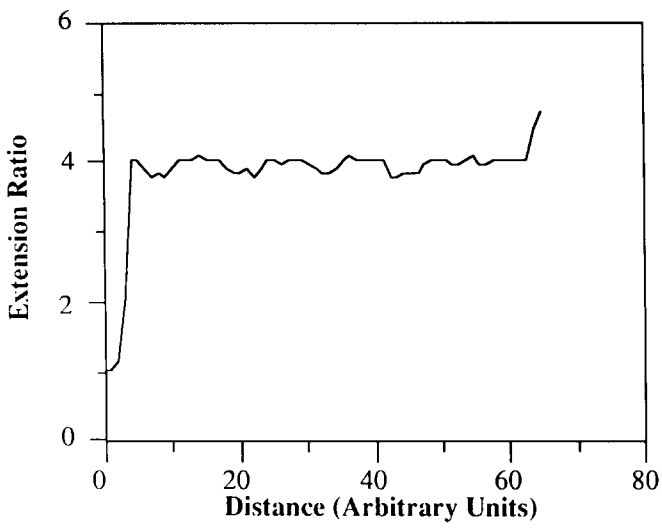

Figure 3 A plot of λ against distance across a RT craze in polydisperse PS $M = 300000$ strained at a strain rate of $10^{-2}\,s^{-1}$ with 5 min intervals between strain increments of 2%

craze, this spread is random whereas the ridges from which δ is determined occur systematically and stretch along the bulk of the craze. As can be seen in *Figure 3*, both λ_{craze} and λ_{ridge} can be characterized with some precision.)

Figure 4 shows an optical micrograph, and a TEM micrograph for comparison, of a DZ in a PES film strained at a strain rate of $10^{-2}\,s^{-1}$ with $t_i = 5$ min. As may be seen, ridges are visible, but less clearly than for the crazes in *Figure 1*, and it was not possible to extract quantitative information on δ from TEM micrographs of PES during densitometry. However, when viewed optically in reflected light the ridges are clearly distinguished from their surroundings by changes in interference colours.

The value of δ can be found from the change in interference colour as follows. For a two-dimensional stretch the local thickness t is related to the original film thickness by $t = t_0/\lambda$. For any thickness t, the wavelength of the interference colour (as estimated using a colour chart) is equal to $2\mu t(n + 1/2)\Lambda$, where n is the order of the colours, μ the refractive index and Λ is the wavelength of the interference colour (as estimated using a colour chart). Therefore the ratio of the extension ratios of two different parts of the specimen is given by:

$$\lambda_2/\lambda_1 = (n_1 + 1/2)\Lambda_1/(n_2 + 1/2)\Lambda_2$$

which reduces to Λ_1/Λ_2 if, as in general, the interference colours are of the same order. Then δ is given simply by $1 - \Lambda_{DZ}/\Lambda_{ridge}$, where Λ_{DZ} and Λ_{ridge} are the wavelengths of the interference colours observed in the DZ body and the ridges respectively. For the conditions corresponding to *Figure 4*, δ was found to be approximately 0.06. Although this is similar to the value found for PS crazes under similar conditions, since λ_{DZ} for PES is approximately 1.3 compared with $\lambda = 4$ for PS, the absolute ridge height is much smaller than in PS crazes, accounting for the relatively poor contrast in the TEM image in *Figure 4*.

Time and temperature effects

Figure 5a shows a TEM micrograph of a craze in PS $M = 300000$ given successive strain increments of 2% at 70°C at a strain rate of $10^{-2}\,s^{-1}$ with various t_i, and *Figure 5b* shows the corresponding variation in λ_{craze}. There are two obvious differences between the behaviour at 70°C and RT. First it is clear that there is a much higher level of contrast between the ridges and the remainder of the craze, that is to say that δ is greater, but as at RT δ decreases with t_i. This is shown clearly in *Figure 5a* where the four ridges correspond to decreasing values of t_i moving away from the midrib. Secondly, there is a sharp rise in λ_{craze} on the midrib side of ridges for large t_i, that is, there is a local increase in λ_{craze} over the value of 4. This local increase can be explained in terms of disentanglement. When straining is stopped, the craze will continue to widen but at a reduced rate as the stress in the film decreases. As the craze widening rate decreases, individual chains spend longer in the strain-softened zone at the craze–bulk interface than when the strain is being increased at a rate of $10^{-2}\,s^{-1}$, i.e. t_r is increased. This means that at elevated temperature the chains are able to slide past one another,

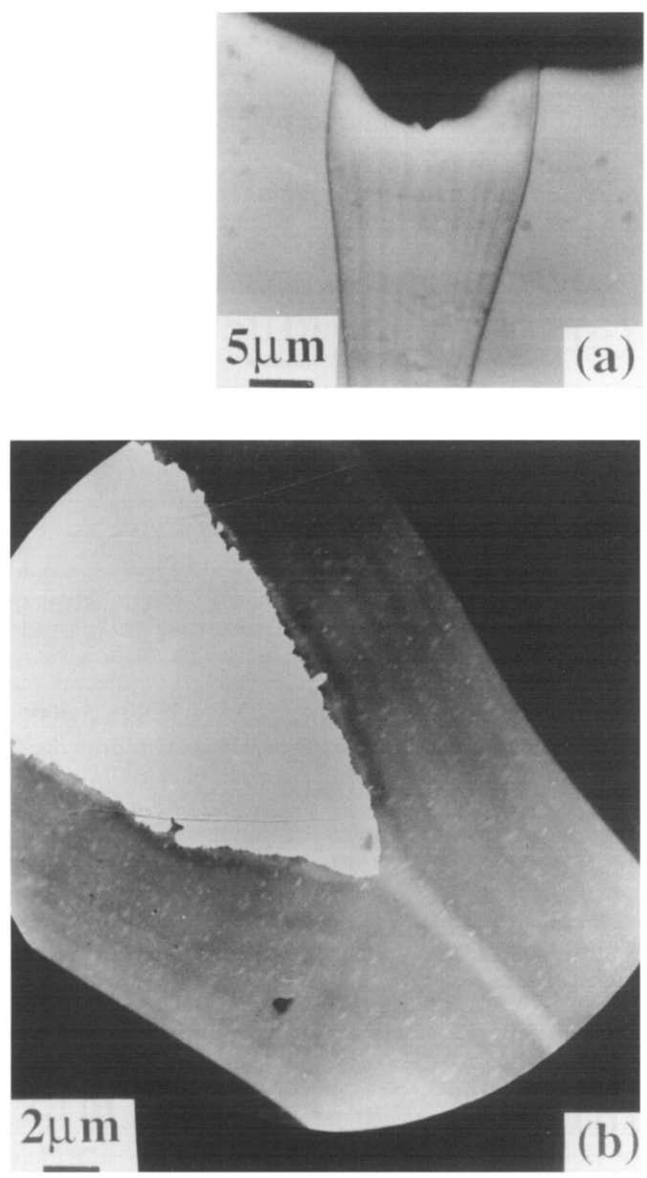

Figure 4 (a) An optical micrograph and (b) a TEM micrograph for comparison of a DZ in a PES film aged for 1 h and step-strained at RT and at a strain rate of $10^{-2}\,s^{-1}$ with 5 min intervals between strain increments of 2%

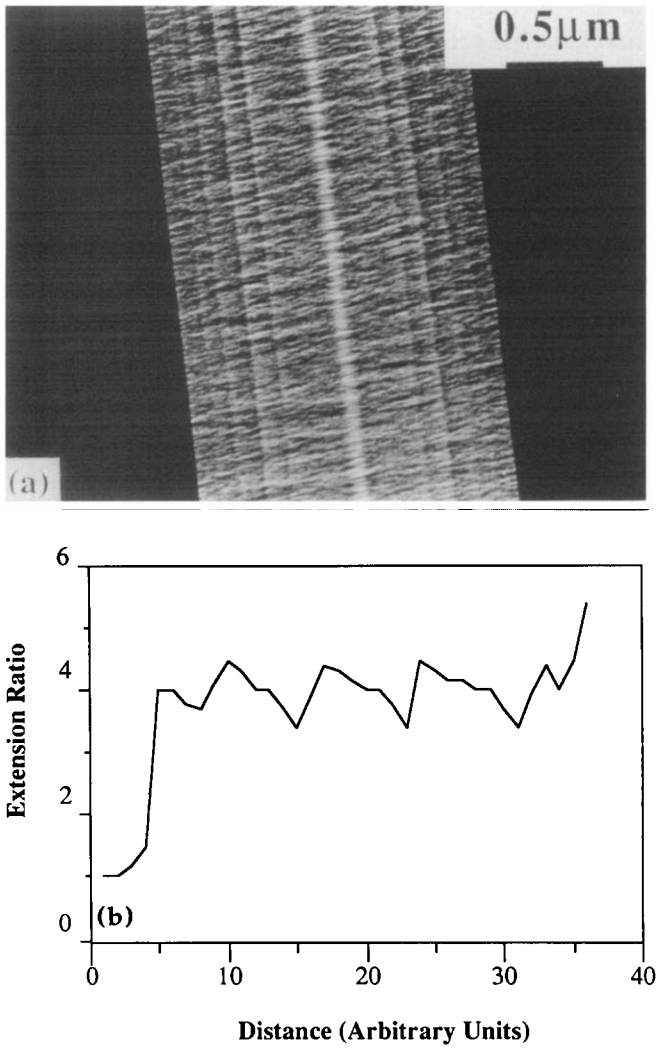

Figure 5 (a) A TEM micrograph of a craze in PS $M = 300\,000$ given successive strain increments of 2% at 70°C at a strain rate of $10^{-2}\,s^{-1}$ with successive intervals between strain increments $t_i = 15$ min, 5 min, 1 min and 30 s; (b) shows the corresponding variation in λ_{craze}

which in turn leads to higher values of λ_{craze} than would be expected on the basis of the fixed entanglement network model. Thus places where the value of λ is locally high correspond to those regions which were able to continue growing after the macroscopically applied strain rate was stopped. The effect of stress ageing localizes this increase and leads to ridges as before, where drawing is less easy than in undeformed, unaged material.

Since we are primarily interested in comparing values of λ_{ridge} with the steady-state value of λ_{craze} during straining, this rise has been ignored and δ has been calculated using the bulk value of λ_{craze}, which remains approximately equal to 4 for steady-state craze widening at elevated temperatures at this strain rate of $10^{-2}\,s^{-1}$. *Figure 6* shows values of δ for different t_i and different temperatures for monodisperse PS $M = 300\,000$. At RT, the value of δ increases approximately as $\log t_i$, reaching 0.17 for $t_i = 12$ h. As the temperature is increased, the initial rate of increase of δ with $\log t_i$ becomes progressively steeper, but appears to flatten off for large t_i, and indeed for the highest temperature, 80°C, δ reaches a maximum of approximately 0.1 for $t_i = 5$ min and then decreases somewhat as t_i is increased, so that δ is approximately 0.08 for $t_i = 1$ h.

Figure 7 shows, for comparison, results for DZs in PES for various temperatures and t_i and a strain rate of $10^{-2}\,s^{-1}$. Again there is an approximate $\log t_i$ dependence of δ and a steeper increase of δ with $\log t_i$ for higher temperatures. Unlike in the PS crazes of *Figure 6*, there is little decrease in the slope of δ against $\log t_i$ with T, although it is significant that even the highest temperature investigated, 70°C, was over 130°C below T_g, whereas in PS the highest temperature investigated was only 20°C below T_g. Measurements at higher temperature were not possible in PES owing to the onset of crazing and film breakdown.

Molecular-weight effects

Figures 8 and *9* show results for monodisperse PS $M = 100\,000$ and polydisperse PS $M_w \sim 100\,000$ for various temperatures and t_i and a strain rate of $10^{-2}\,s^{-1}$. The qualitative behaviour is similar to that observed in PS $M = 300\,000$, but the tendency for δ to show a maximum as a function of t_i as the temperature is

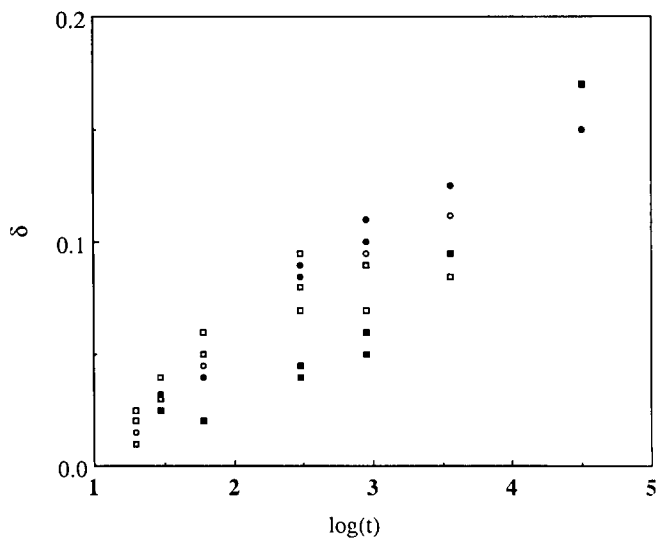

Figure 6 Plot of δ for different t_i and different temperatures for crazes in monodisperse PS $M = 300\,000$ strained at a strain rate of $10^{-2}\,s^{-1}$: (■) RT; (○) 50°C; (●) 70°C; (□) 80°C

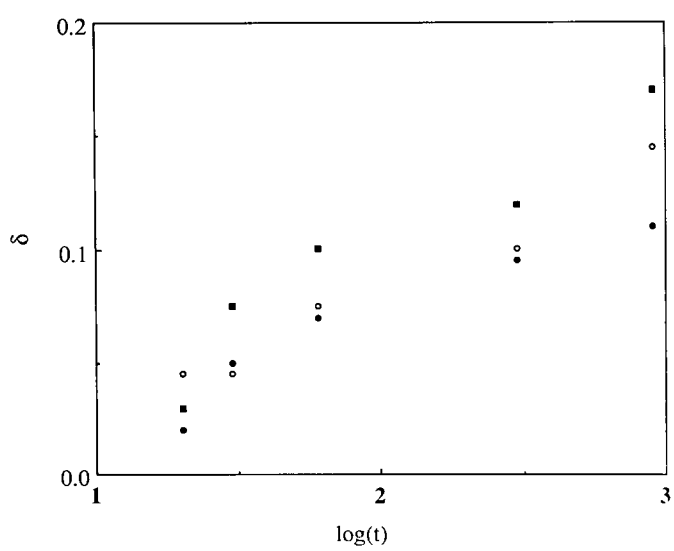

Figure 7 Plot of δ for different t_i and different T for DZs in PES for various temperatures and t_i and a strain rate of $10^{-2}\,s^{-1}$: (●) RT; (○) 50°C; (■) 70°C

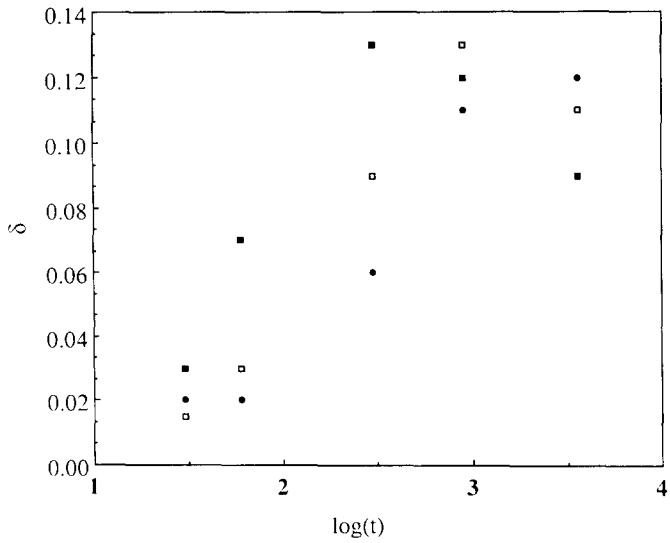

Figure 8 Plot of δ for different t_i and different temperatures for crazes in monodisperse PS $M = 100\,000$ strained at a strain rate of $10^{-2}\,s^{-1}$: (●) RT; (□) 40°C; (■) 60°C

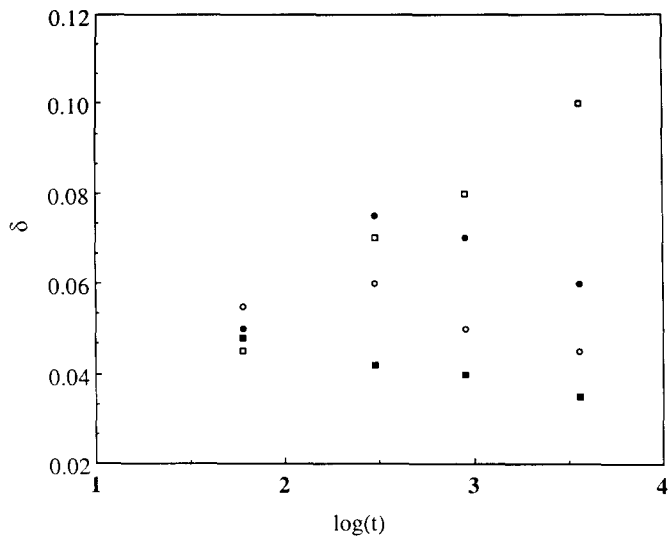

Figure 9 Plot of δ for different t_i and different temperatures for crazes in monodisperse PS $M = 100\,000$ strained at a strain rate of $10^{-2}\,s^{-1}$: (□) RT; (●) 40°C; (○) 50°C; (■) 60°C

increased is more marked (note that craze breakdown restricted the range of temperature in which data could be obtained for low-molecular-weight PS). For the monodisperse PS $M = 100\,000$ there is a peak in δ for $t_i = 15$ min at 40°C, whereas at 60°C δ peaks at $t_i = 5$ min. Hence the peak in δ appears to move to lower t_i as the temperature is raised. For the polydisperse PS $M_w \sim 100\,000$, there is a peak in δ for $t_i = 5$ min at 40°C, and by 60°C, δ appears to peak for $t_i \leqslant 1$ min.

No systematic changes in the behaviour of PES DZs was found with M_w, probably because only a narrow range of M_w was available (47 000 to 69 000), and all samples were polydisperse.

Strain-rate effects

The effect of step-straining at a strain rate of $4 \times 10^{-6}\,s^{-1}$ for similar ranges of t_i and temperature to those described above, and for molecular weights of PS up to $M = 1\,150\,000$, was also investigated. Little evidence of step-strain ridges was found during these measurements and δ could not be quantified either for PS crazes or for PES DZs. *Figure 10* shows, for example, a craze in PS $M = 1\,150\,000$ step-strained at RT at a strain rate of $4 \times 10^{-6}\,s^{-1}$, with $t_i = 1$ h.

In some experiments carried out at a strain rate of $10^{-2}\,s^{-1}$, rather than dropping the strain rate to zero in the time interval between each strain increment, it was dropped to $4 \times 10^{-6}\,s^{-1}$. In such samples, ridges resulted that were identical (same δ), within the limits of experimental error, with those which resulted when the strain rate was reduced to zero between strain increments. This was true both of crazes in PS and of DZs in PES.

DISCUSSION

The ageing process is generally assumed to be one of thermally/stress-activated relaxation. In the appendix it is shown that relaxation kinetics are anticipated to be logarithmic with time (so that after any given time t_i the extent of relaxation will be proportional to $\log t_i$), and also approximately linearly dependent on temperature. It is further shown in the appendix that the quantity δ, which represents the evolution of the ridge height with t_i, can be approximated by an expression proportional to $g_1(t_i)$, where $g_1(t_i)$ represents the cumulative effect of ageing on the yield stress. It follows that a $\log t_i$ dependence for g_1 is to be expected, with an increased ageing rate as temperature is raised. This conclusion appears to be in qualitative accord with the behaviour for a strain rate of $10^{-2}\,s^{-1}$ shown by DZs in PES, and crazes in PS at low temperature and small t_i, as shown by *Figures 6–9*. One would also expect the width of the step-strain ridges to increase with time, but this increase may be offset by further craze widening during stress ageing, which will tend to draw material away from the high-λ part of the neck, and is not obvious from the results presented here. A more quantitative treatment of the results would have to take into account changes in the local stresses and strain rates in more detail. As pointed out by Kramer[13], such modelling is complicated in the case of isometric stress ageing by uncertainties in the nominal stress σ_0 at a given t_i. (Note, however, that, if the craze surface stress were to drop substantially during the duration of our tests, the crazes would begin to close; whereas Wool and O'Connor[25] have reported craze closure below T_g in PS for sufficiently long times,

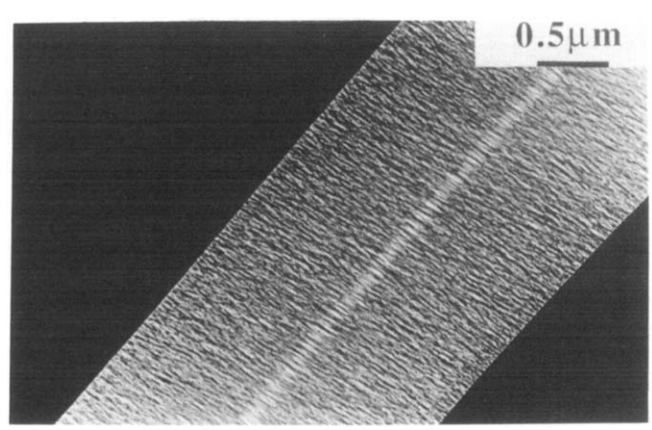

Figure 10 A craze in PS $M = 1\,150\,000$ step-strained at RT at a strain rate of $4 \times 10^{-6}\,s^{-1}$ with $t_i = 1$ h

no sign of craze closure was found under the experimental conditions described here.)

In the low-strain-rate tests it appears that the drawing rate is sufficiently low that a substantial amount of relaxation is able to take place during drawing, so that the ridges formed durng the high-strain-rate tests are suppressed even for t_i as long as 12 h. This is not surprising if one bears in mind that, at this strain rate, the time to increment the strain in the samples by 2% is approximately 1.5 h, that is, much larger than the typical timescales for which we have observed ageing effects during high-strain-rate tests. (It should be noted that, at high strain rates, the time for this strain increment to occur corresponds to the craze widening by an amount similar to the width of the ridges themselves, so that it is possible to distinguish clearly between successive ridges.) In general, there will be a dynamic equilibrium between flow-induced perturbations in the local molecular arrangement, and molecular arrangement characteristic of the relaxed state. At low strain rates, for which more time is available to relax the disruption caused by the molecular rearrangements that arise during flow, one therefore expects that the overall molecular configuration will be much closer to that of the relaxed state than it will be during flow at high strain rates. This can explain the apparent lack of ageing effects in our low-strain-rate tests. The fact that reducing the strain rate from $10^{-2}\ s^{-1}$ to $4 \times 10^{-6}\ s^{-1}$ results in ridges identical to those produced when the strain rate is reduced to zero, also suggests that material being deformed at the low strain rate is relaxing analogously to the ageing that occurs after straining is stopped.

There remains a serious difficulty with a treatment based on a fixed entanglement network model in that it cannot account for the drop in δ in PS for high T, low M and long t_i. The M and t_i dependences suggest that the effect is due to a disentanglement mechanism, that is, one involving the relative motion of whole polymer chains. Under these conditions the entanglement network can no longer be considered permanent, which in turn implies changes in the term $f(\lambda)$ (see appendix) over the duration of the measurements. Such a disentanglement mechanism is likely to be favoured by high chain mobilities and hence high T, consistent with the experimental results for PS.

A similar explanation has also been advanced for observations of the shrinkage stress in glassy polymers as a function of time[26]. In these experiments oriented samples were held at elevated temperature with their ends fixed, and it was found that under these conditions the stress at the sample ends gradually increased from zero. For sufficiently long times and high temperature, the stress reached a maximum and then began to fall (this was observed for polycarbonate (PC) at 110°C after times of the order of 10^5 s). The initial behaviour may be interpreted as the transfer of entropic forces to the surrounding continuum owing to the relaxation of internal stresses. However, for long times, the orientation that gives rise to the entropic forces is itself able to relax by reptation, although there are at present no shrinkage measurements in the glassy state to test the molecular-weight scaling that this implies.

In the results presented here, there are many complicating factors. First, the orientation is localized in the neck. To some extent, Kramer's model for disentanglement[18] takes into account this localization of orientation and stress. The chains are presumed to disentangle by a reptation mechanism (but not classical reptation due to Brownian motion[18,22]) in which the local increase in λ results in a continual relaxation of the entanglement constraint (in contrast, in the Doi–Edwards model λ cannot increase locally since the orientation is assumed to be homogeneous). In this case the disentanglement time τ_{dis} is predicted to scale as M^2.

Secondly, in the case of the PS crazes, the state of the chains in the necks is not well known, because the crazing is accompanied by a considerable amount of chain scission[2]. Since the radius of gyration of the intact chains is of the same order as the fibril separation, and therefore likely to be of the same order as the micro-necks at the craze–bulk interface, then molecular-weight degradation will be effective throughout these necks. Further, although the final molecular weight in the fully formed craze fibrils may be estimated[2], this may differ considerably from the molecular weight corresponding to intermediate stages of fibril formation. Nevertheless, one may assume that a large starting M will in general give a relatively high effective fibrillar molecular weight.

Finally, there is the additional problem of polydispersity. Since the presence of small relatively mobile chains leads to relaxation of the tube constraints, and hence a weakening of the apparent M dependence, one would expect polydispersity to promote disentanglement. The results confirm this expected behaviour. However, even for samples that are initially monodisperse, scission will lead to a broadening of the molecular-weight distribution in the neck region, leading to the possibility of such tube relaxation occurring. Hence the net effect will lead to an expectation that the peaks in the $\delta(t_i)$ curves should appear at lower t_i as the starting molecular weight is decreased and as the temperature is increased, consistent with the results, but it is not possible to make a quantitative prediction of the associated molecular-weight scaling.

We interpret the overall qualitative behaviour of the crazes as follows. As the craze widens, deformation is initially restricted to an 'active zone' of strain-softened polymer at the craze–bulk interface. At low temperature and for large M the entanglement network may be considered fixed so that the fibril extension ratio λ is a function of the initial entanglement network parameters and the craze geometry only. However, for sufficiently high temperature and/or high stresses, additional entanglement loss may occur owing to chain slip, or disentanglement, in the strain-softened region, leading to an increase in λ, and ultimately, at very high temperature or stress, fibril breakdown at the craze–bulk interface. Beyond a certain time (20 s in *Figure 1*) however, the mobility of chains initially in the strain-softened state will decrease owing to stress ageing, so that regions of the fully formed fibril become stable, that is, there are no further changes in λ. In this case ridges are left if the strain rate is increased again. Nevertheless, since the rate of ageing decreases with time, for sufficiently long times disentanglement may become effective once more for chains in the stress-aged state. This 'secondary' disentanglement appears to be responsible for the apparent softening effect we have observed, and the suppression of the step-strain ridges in our samples for relatively long ageing times leading to a decrease in δ. This onset of disentanglement in the strain-hardened state is also expected to give rise to fibril creep, so that, as temperature

is increased or M is decreased, there may be an increased tendency for craze breakdown, although this will also depend on the extent to which the craze surface stresses decrease as a result of bulk relaxation during the heat treatment. Where fibril creep is taking place, breakdown would tend to initiate at the craze midrib or at the craze tips, where the true stress is relatively high, rather than the craze–bulk interface, since it is not dependent on there being strain softening[18]. However, further work is required to test this prediction.

CONCLUSIONS

We have found that for relatively short ageing times and at relatively low temperatures, 'step-strain ridges' observed in crazes in PS and in DZs in PES formed at a strain rate of $10^{-2}\,s^{-1}$ become more marked as the interval t_i between successive strain increments is increased. This effect can be related to the phenomenon of stress ageing, as suggested by the approximate logarithmic dependence of δ on t_i, where δ represents the ridge height. This type of dependence makes it difficult to characterize these ageing effects in terms of a single time constant, as assumed in Kramer and Berger's choice of a single parameter t_r to characterize age hardening in their model for craze breakdown by reptation[21]. Moreover, at low strain rates similar to those at which Kramer and Berger's data were obtained ($4 \times 10^{-6}\,s^{-1}$), we were in fact unable to observe any stress ageing effects. (It is perhaps worth pointing out, however, as did Kramer and Berger, that additional factors such as recombination of free radicals of the broken chain ends may be relevant to craze breakdown.)

At high temperatures, and for low-molecular-weight samples and relatively long t_i, the value of the ridge height obtained in high-strain-rate tests may begin to *decrease* with t_i. In view of the molecular-weight dependence, this has been argued to be a consequence of disentanglement in the aged material leading to a gradual increase in the local extension ratio. We speculate on this basis that at very high temperatures fibrillar creep may become the relevant mechanism for breakdown in low-molecular-weight materials.

ACKNOWLEDGEMENT

We are grateful to ICI plc for funding this work.

REFERENCES

1 Donald, A. M. and Kramer, E. J. *J. Polym. Sci., Polym. Phys. Edn.* 1982, **20**, 899
2 Kramer, E. J. 'Advances in Polymer Science', Vol. 52/53 (Ed. H. H. Kausch), Springer-Verlag, Berlin, 1983, Ch. 1
3 Donald, A. M. and Kramer, E. J. *J. Mater. Sci.* 1981, **16**, 2967
4 Donald, A. M. and Kramer, E. J. *Polymer* 1982, **23**, 461
5 Fellers, J. F. and Kee, B. F. *J. Appl. Polym. Sci.* 1974, **18**, 2355
6 Donald, A. M. *J. Mater. Sci.* 1985, **20**, 263
7 Plummer, C. J. G. and Donald, A. M. *J. Polym. Sci., Polym. Phys. Edn.* 1989, **27**, 235
8 Kramer, E. J. *Polym. Eng. Sci.* 1984, **24**, 761
9 Kuo, C. C., Phoenix, S. L. and Kramer, E. J. *J. Mater. Sci. Lett.* 1985, **4**, 459
10 Lauterwasser, B. D. and Kramer, E. J. *Phil. Mag.* 1979, **39a**, 469
11 Chan, T., Donald, A. M. and Kramer, E. J. *J. Mater. Sci.* 1981, **16**, 676
12 Donald, A. M. and Kramer, E. J. *Polymer* 1982, **23**, 457
13 Kramer, E. J. *J. Appl. Phys.* 1970, **47**, 4327
14 Richards, R. MS Thesis, Cornell University, 1971
15 Struik, L. C. E. 'Physical Ageing in Amorphous Polymers and Other Materials', Elsevier, Amsterdam, 1975
16 Ricco, T. and Smith, T. L. *Polymer* 1985, **26**, 1979
17 Smith, T. L. and Haidar, B. Proc. 7th Int. Conf. on Deformation, Yield and Fracture of Polymers, Cambridge, 1988, Paper 1
18 Kramer, E. J. and Berger, L. L. *Adv. Polym. Sci.* 1990, **91/2**, 1
19 DeGennes, P. G. *J. Chem. Phys.* 1971, **55**, 572
20 Doi, M. and Edwards, S. F. *J. Chem. Phys.* 1971, **55**, 1789, 1802
21 Berger, L. L. and Kramer, E. J. *Macromolecules* 1987, **20**, 1980
22 McLeish, T. C. B., Plummer, C. J. G. and Donald, A. M. *Polymer* 1989, **30**, 1651
23 Chan, T., Donald, A. M. and Kramer, E. J. *J. Mater. Sci.* 1981, **16**, 676
24 Donald, A. M. and Kramer, E. J. *J. Mater. Sci.* 1982, **17**, 1871
25 Wool, R. P. and O'Connor, K. M. *Polym. Eng. Sci.* 1981, **21**, 970
26 Pakula, T. and Trznadel, M. *Polymer* 1985, **26**, 1011
27 Evetts, J. E. in 'Rapidly Quenched Metals' (Eds. S. Steeb and H. Warlimont), Elsevier, Amsterdam, 1985, p. 607
28 Evetts, J. E. personal communication

APPENDIX

In a spatially inhomogeneous system such as a glass, there will be a corresponding variation in the local activation energy. The glass can be characterized as an assembly of two-level systems (the two levels corresponding to relaxed and unrelaxed states), with a corresponding activation energy spectrum $Q(E)$[27]. Changes in the property that is being relaxed then reflect the number of states that have crossed the activation barrier after a given time t_i (this is consistent with an Eyring model for yield, for example, where changes in the yield stress are proportional to changes in the mean activation energy). States that are relaxing at time t_i will be those for which $t_i = \tau(E)$, where the relaxation time $\tau(E)$ is given by $\tau = \nu^{-1}\exp(E/kT)$; ν is a frequency factor. For a broad activation spectrum, the density of states $Q(E)$ may be assumed independent of E and therefore approximated by a top-hat function over a large range of τ so that the extent of relaxation in a time interval t within this range of τ is proportional to $Q\,\Delta E$ (ref. 28). This expression is in turn proportional to $kT\log(t_i/t_0)$, where t_0 is a constant which depends on the initial state of the material. Thus in general, $\log(t_i)$ kinetics may be anticipated for relaxation in the glassy state. The stress ageing rate will also increase with T, although the linear dependence implied here is an oversimplification, which does not, for example, take into account any temperature dependence of E.

A simple multiplicative constitutive equation for the post-yield behaviour of the glassy polymer is assumed, which takes the form:

$$\sigma_f = \kappa f(\lambda) g_0(\dot{\varepsilon}) \qquad \text{(A1)}$$

where σ_f is the flow stress, κ is a scaling factor and $g_0(\dot{\varepsilon})$ shows power-law behaviour, such that $m = [\partial \ln \sigma_f / \partial \ln \dot{\varepsilon}]_\lambda$, the strain-rate sensitivity, is of the order of 0.1 (ref. 2). The term $f(\lambda)$ reflects the contribution to σ_f from entropic hardening at an extension ratio of λ, and for a fixed entanglement network will therefore become infinite as λ approaches λ_{max} (where λ_{max} represents the state where the polymer strands between entanglement points are fully extended and for the sake of argument is assumed to give the bulk craze extension ratio). For a neck propagating in the steady state at a nominal flow stress σ_{0f}, the following will hold within the neck:

$$\sigma_{0f} = \frac{\sigma_f}{\lambda} = \frac{\kappa}{\lambda} f(\lambda) g_0(\dot{\varepsilon}) \qquad \text{(A2)}$$

where the local strain rate $\dot{\varepsilon}$ is determined by the sample extension rate and the neck geometry. During stress ageing at a constant sample extension and for a fixed entanglement network, the term $f(\lambda)$ should be independent of time. Therefore any development of a yield stress must be taken up by changes in $g(\dot{\varepsilon})$ (where $\dot{\varepsilon}$ refers to the local strain rate on resumption of the original sample deformation rate). The term $g(\dot{\varepsilon})$ may be written as $g_0(\dot{\varepsilon}) + g_1(t_i, \lambda)$; the λ dependence reflects the variation in the local stress ageing rate with the local stress, which will be equal to $\lambda\sigma_0$ for a given nominal stress σ_0. The local nominal yield stress is then:

$$\sigma_{0y} = \frac{\sigma_y}{\lambda} = \frac{\kappa}{\lambda} f(\lambda)[g_0 + g_1(t_i, \lambda)] = \sigma_{0f}\left(1 + \frac{g_1(t_i, \lambda)}{g_0}\right) \tag{A3}$$

When the stress in the sample is raised on restoration of the original sample deformation rate, because g is an increasing function of λ, yielding will take place initially at the site of the bulk–neck interface where λ is close to unity (and σ_{0y} is relatively low). The newly formed region of instability will then propagate into the undeformed bulk and (potentially) into the original necked region simultaneously, and the nominal stress will drop towards σ_{0f} once again.

However, under these conditions, the maximum stress in the sample will approach $\lambda_{max}\sigma_{0f}$ and so, to a first approximation, regions of the original neck for which $\lambda_{max}\sigma_{0f}$ is less than $\lambda_c\sigma_{0y}$, with σ_{0y} given by equation (A3), will not yield on resumption of straining. This condition may be written:

$$\lambda_{max} \leqslant \lambda_c\left(1 + \frac{g_1(t_i, \lambda)}{g_0}\right) \tag{A4}$$

where λ_c is a critical value for λ such that regions of the original neck for which $\lambda > \lambda_c$ will not undergo yield. For finite g_1 then a ridge for which $\lambda_c < \lambda < \lambda_{max}$ will be left behind as the new neck continues to propagate into the bulk.

Since the measured extension ratio of the ridges varies relatively little (showing a maximum deviation from the bulk craze extension ratio of 20% over several decades of t_i), we assume that changes in g_1 are dominated by $\log t_i$ and ignore its λ dependence. Hence, using (A4) to substitute for λ_c in our expression for δ, we have:

$$\delta = \frac{\lambda_{max} - \lambda_c}{\lambda_{max}} \simeq \frac{g_1(t_i)}{g_0 + g_1(t_i)} \simeq \frac{g_1(t_i)}{g_0} \tag{A5}$$